OPTIMIZED PERFORMANCE OF A MOTOR-BEARING

Rafael Ramos Gomes, EE.
Laboratório de Aplicações de Supercondutores (UFRJ)
Centro de Tecnologia – I 148, Cidade Universitária - Caixa Postal 68504
CEP 21945-970 - Rio de Janeiro - RJ - Brasil.
ramos@ufrj.br

José Andrés Santisteban, D.Sc.
Universidade Federal Fluminense (UFF)
Escola de Engenharia/TEE/PGMEC, Rua Passo da Pátria, 156
CEP 24210-240 - Niteroi - RJ - Brazil
jasantisteban@vm.uff.br

Richard Magdalena Stephan, Dr.-Ing.
Laboratório de Aplicações de Supercondutores (UFRJ)
Centro de Tecnologia – I 148, Cidade Universitária - Caixa Postal 68504
CEP 21945-970 - Rio de Janeiro - RJ – Brasil.
rms@ufrj.br

Abstract. *The purpose of this work is to describe a bearingless machine prototype developed at UFRJ. An electromagnetic model and a mechanical model are presented. Based on these models, a mathematical simulation study was carried out. PD´s controllers are used for feedback control stabilization. Simulations results validate the models.*

Keywords*: Electrical Machines, Magnetic Bearings, Feedback Control Systems, System Modeling, Mathematical Simulations, Emerging Technologies.*

1. Introduction

Magnetic bearings are nowadays employed in some industrial machines, replacing the conventional mechanical bearings. The main function of those magnetic bearings is to support the rotating part (rotor) without contacting the stator. This technology eliminates mechanical friction and the need of lubrication. This characteristic also allows motor operation at high rotating speeds where the use of conventional mechanical bearings would be forbidden.

Magnetic bearings can be classified in two broad types:

- passive bearing and
- actively controlled bearing.

Passive magnetic bearings employ permanent magnets, which generate positioning forces but cannot stabilize the rotor in all degrees of freedom (Earnshaw, 1842). Another passive technique is based on the diamagnetic property of superconducting materials and has the advantage of being intrinsically stable.

Active bearings employ some kind of electronic feedback. The electromagnetic bearing falls in this category. Position sensors acquire the rotor shaft position that is compared with a reference air gap value (Santisteban et al, 1997, 1999, and David, 2003). The processed error signal adjusts the current intensity flowing through an electromagnetic positioning winding (see Fig. 1). Figure 2 illustrates a set of two radial magnetic bearings and an axial one necessary to the operation of an electric machine.

The volume of this hole system can be reduced if the machine winding currents are used for the production of both the rotation and the positioning of the rotor. This scheme is called motor-bearing. The present paper describes a mathematical model of this system. Based on this model, simulation studies allow the selection of an optimized controller to stabilize the shaft position.

2. Electromagnetic model

The electromagnetic equations that govern a motor-bearing can be derived from Fig 3. The equivalent magnetic circuit is given in Fig. 4.

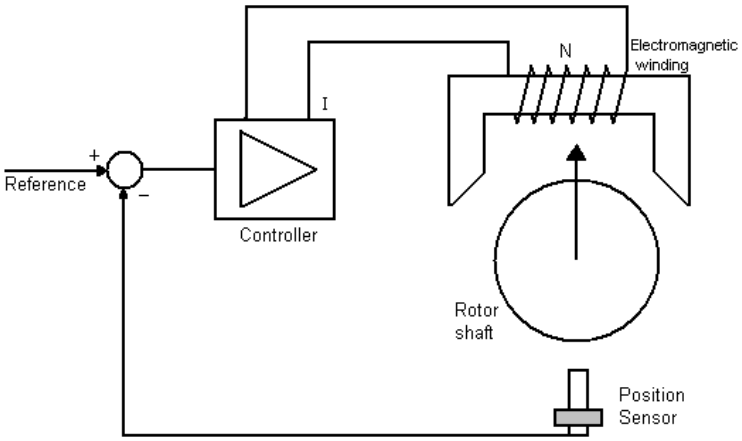

Figure 1. Operation principles of an electromagnetic bearing.

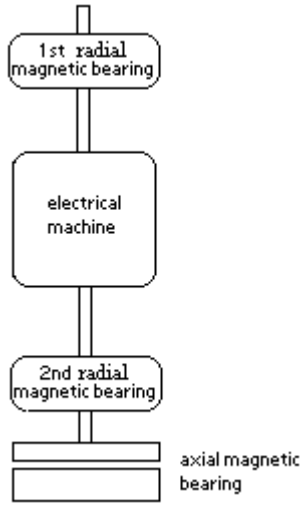

Figure 2.Set of conventional magnetic bearings.

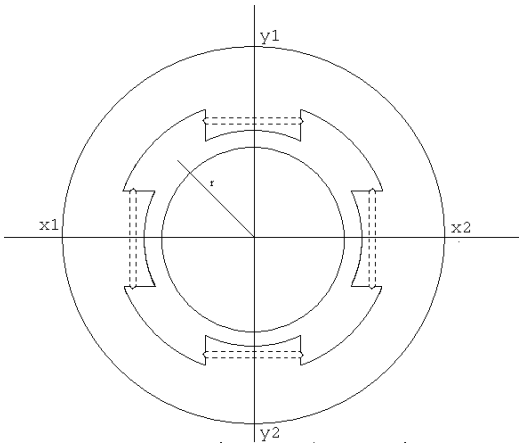

Figure 3. Equivalent magnetic scheme.

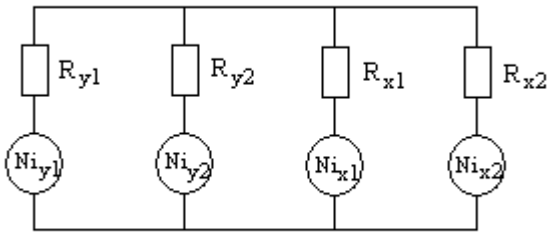

Figure 4. Magnetic circuit.

The linked flux relates with the currents by Eq. (1). Assuming the equivalent reluctance is given by Eq. (2), the inductance matrix can be written by Eq. (3).

$$[\lambda] = [L(h)][I] \tag{1}$$

$$\frac{1}{R_{eq}} = \frac{1}{R_{y1}} + \frac{1}{R_{y2}} + \frac{1}{R_{x1}} + \frac{1}{R_{x2}} \tag{2}$$

$$\begin{bmatrix}\lambda_{y1}\\ \lambda_{y2}\\ \lambda_{x1}\\ \lambda_{x2}\end{bmatrix} = N^2 \begin{bmatrix} \frac{1}{R_{y1}} - \frac{R_{eq}}{R_{y1}^2} & -\frac{R_{eq}}{R_{y1}R_{y2}} & -\frac{R_{eq}}{R_{y1}R_{x1}} & -\frac{R_{eq}}{R_{y1}R_{x2}} \\ -\frac{R_{eq}}{R_{y2}R_{y1}} & \frac{1}{R_{y2}} - \frac{R_{eq}}{R_{y2}^2} & -\frac{R_{eq}}{R_{y2}R_{x1}} & -\frac{R_{eq}}{R_{y2}R_{x2}} \\ -\frac{R_{eq}}{R_{x1}R_{y1}} & -\frac{R_{eq}}{R_{x1}R_{y2}} & \frac{1}{R_{x1}} - \frac{R_{eq}}{R_{x1}^2} & -\frac{R_{eq}}{R_{x1}R_{x2}} \\ -\frac{R_{eq}}{R_{x2}R_{y1}} & -\frac{R_{eq}}{R_{x2}R_{y2}} & -\frac{R_{eq}}{R_{x2}R_{x1}} & \frac{1}{R_{x2}} - \frac{R_{eq}}{R_{x2}^2} \end{bmatrix} \begin{bmatrix} i_{y1}\\ i_{y2}\\ i_{x1}\\ i_{x2}\end{bmatrix}. \tag{3}$$

The inductance matrix is a function of the radial displacement, where each reluctance is calculated by Eq. (4):

$$R = \frac{h}{\mu A}. \tag{4}$$

where: μ is the air permeability constant; h is the correspondent air gap (y_1, y_2, x_1, x_2) and A is the mean area of each magnetic pole.

The stored magnetic energy (W_e) inside the air gap in given by Eq. (5), and the radial forces (F_e) are calculated from the derivatives of this energy as explained in Eq. (6) and Eq. (7).

$$W_e = \frac{1}{2}[i]^T [L(h)][i], \tag{5}$$

$$F_e = \frac{dW_e}{dh}, \tag{6}$$

$$F_e = \frac{1}{2}[i]^T \frac{d[L(h)]}{dh}[i], \tag{7}$$

Using the transformations: $y_1 = y = h_0 + \Delta y$; $y_2 = (2h_0 - y) = h_0 - \Delta y$; $x_1 = x = h_0 + \Delta x$; $x_2 = (2h_0 - x) = h_0 - \Delta x$, where h_0 is the nominal air gap in the centered condition, the first term of the inductance matrix $L_{11}(h)$ will be:

$$L_{11} = \mu A N^2 \left[\frac{1}{y} - \frac{1}{2h_0\left(\frac{y^2}{x(2h_0 - x)} + \frac{y}{(2h_0 - x)} \right)} \right]. \tag{8}$$

The other terms of the inductance matrix can be calculated analogously. The derivative of $[L(h)]$ with respect to the displacement y_1 is given by Eq. (9). After some simplifications, it follows:

$$\frac{\partial[L(h)]}{\partial y_1} = -\frac{1}{2} N^2 \mu \frac{A}{y^2} \begin{bmatrix} 1 & 0 & -\frac{1}{2} & -\frac{1}{2} \\ 0 & -1 & \frac{1}{2} & \frac{1}{2} \\ -\frac{1}{2} & \frac{1}{2} & 0 & 0 \\ -\frac{1}{2} & \frac{1}{2} & 0 & 0 \end{bmatrix}. \tag{9}$$

The equivalent force along direction y_1 is determined using Eq. (7) as:

$$F_{y1} = -\frac{1}{4} N^2 \mu \frac{A}{y^2} \left[{i_{y1}}^2 - {i_{y2}}^2 + (i_{y2} - i_{y1})(i_{x1} + i_{x2}) \right]. \tag{10}$$

Analogously, $\frac{\partial [L(h)]}{\partial y_2}$ can be calculated. The equivalent force along direction y_2 is expressed by Eq. (11):

$$F_{y2} = -\frac{1}{4} N^2 \mu \frac{A}{y^2} \left[{i_{y2}}^2 - {i_{y1}}^2 + (i_{y1} - i_{y2})(i_{x1} + i_{x2}) \right]. \tag{11}$$

The forces along the "*x*" axis can also, in the same way, be obtained.
The currents imposed have the following expressions:

$$i_{y1} = (i_0 + \Delta i_y) \cos \omega t \,, \tag{12}$$
$$i_{y2} = (i_0 - \Delta i_y) \cos \omega t \,, \tag{13}$$
$$i_{x1} = (i_0 + \Delta i_x) \cos \omega t \,, \tag{14}$$
$$i_{x2} = (i_0 - \Delta i_x) \cos \omega t \,. \tag{15}$$

where: i_0 is a mean value, determined by a particular stiffness for the magnetic bearing, and Δi is the incremental value supplied by the position control.

Now Eqs. (10) and (11) can be rewritten as:

$$F_{y1} = -\frac{1}{4} N^2 \mu \frac{A}{y^2} \left[8 i_0 \Delta i_y \right] \cos^2 \omega t \,, \tag{16}$$

$$F_{y2} = -\frac{1}{4} N^2 \mu \frac{A}{y^2} \left[-8 i_0 \Delta i_y \right] \cos^2 \omega t \,, \tag{17}$$

The force can be considered directly proportional to Δi_y for small displacements (y approximately constant).
The term $\cos^2 \omega t$ can also be decomposed in:

$$\cos^2 \omega t = \frac{1}{2} (1 + \cos 2\omega t), \tag{18}$$

showing two components:

- a continuous force and
- an harmonic force.

As long as the natural frequencies of the rotor are kept reasonably lower than the harmonic frequency, the oscillatory term will produce a negligible effect on the dynamic behavior of the system.

3. Mechanical Model

A schematic drawing of a vertical rotor pivoted on a point "O" is shown in Fig. 5 as described in Santisteban, 1999. Since the rotor is considered to be pivoted at the lower bearing, only the magnetic bearing forces acting at an axial distance "*b*" from "O" contribute to the mechanical positioning of the rotor.

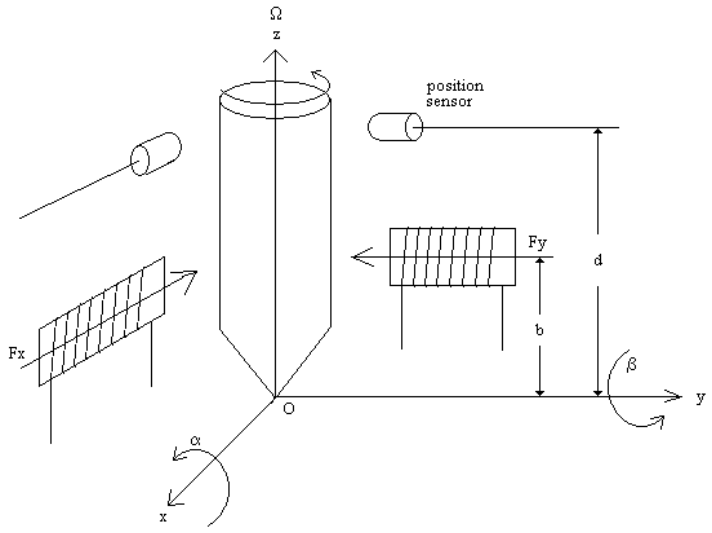

Figure 5. Mechanical model.

Assuming that the system has two degrees of freedom, the following equation may be written:

$$\begin{bmatrix} I_0 & 0 \\ 0 & I_9 \end{bmatrix} \begin{Bmatrix} \ddot{\alpha} \\ \ddot{\beta} \end{Bmatrix} + \begin{bmatrix} 0 & -I_p\Omega \\ I_p\Omega & 0 \end{bmatrix} \begin{Bmatrix} \dot{\alpha} \\ \dot{\beta} \end{Bmatrix} = \begin{Bmatrix} -bF_y \\ bF_x \end{Bmatrix} . \tag{19}$$

where I_0 is the transversal moment of inertia at point "O", I_p is the moment of inertia of the rotor and Ω its spin velocity.

From a control point of view, it is convenient to express Eq. (19) in terms of the radial displacement coordinates "x" and "y" provided by the displacement sensors positioned at an axial distance "d" from the pivot point "O". Assuming that the angular displacements $\alpha = -y/d$ and $\beta = x/d$ are small, Eq. (19) in terms of "x" and "y" is:

$$\begin{bmatrix} I_0 & 0 \\ 0 & I_9 \end{bmatrix} \begin{Bmatrix} \ddot{y} \\ \ddot{x} \end{Bmatrix} + \begin{bmatrix} 0 & -I_p\Omega \\ I_p\Omega & 0 \end{bmatrix} \begin{Bmatrix} \dot{y} \\ \dot{x} \end{Bmatrix} = \begin{Bmatrix} bdF_y \\ bdF_x \end{Bmatrix} . \tag{20}$$

This matrix equation can be written as system of two differential equations:

$$\ddot{x} = \frac{I_p}{I_0}\Omega\dot{y} + \frac{bd}{I_0}F_x , \tag{21}$$

$$\ddot{y} = -\frac{I_p}{I_0}\Omega\dot{x} + \frac{bd}{I_0}F_y . \tag{22}$$

The moments of inertia I_0 and I_p of the laboratory prototype were measured:
I_0= 0.134078 kg-m^2,
Ip= 0.003996 kg-m^2,
while the heights "*b*" and "*d*" are: *b*= 0.195 m, *d*= 0.345 m.

Talking these values into account, Eqs. (21) and (22) lead the block diagram shown in Fig. 6.

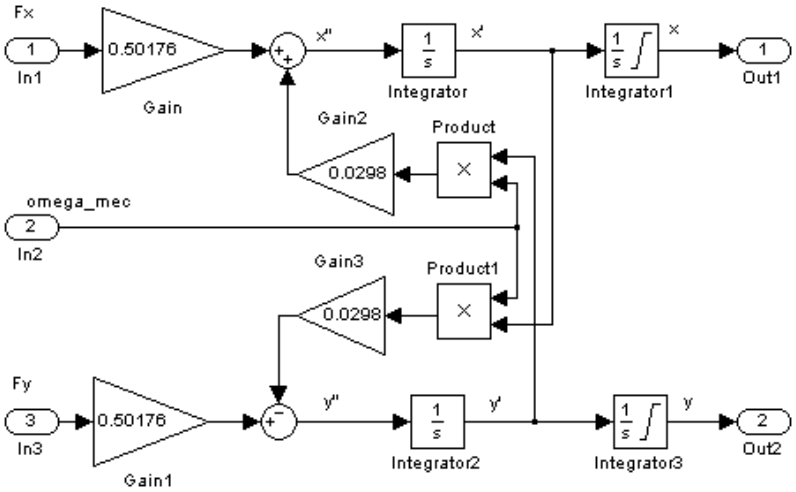

Figure 6. Block diagram of the mechanical model.

The integrator1 and integrator3 in Fig. 6 have saturations to represent the physical system.

4 Simulations

According to the mechanical and electromagnetic models presented in the previous sections, the simulation model shown in Fig. 7 is obtained.

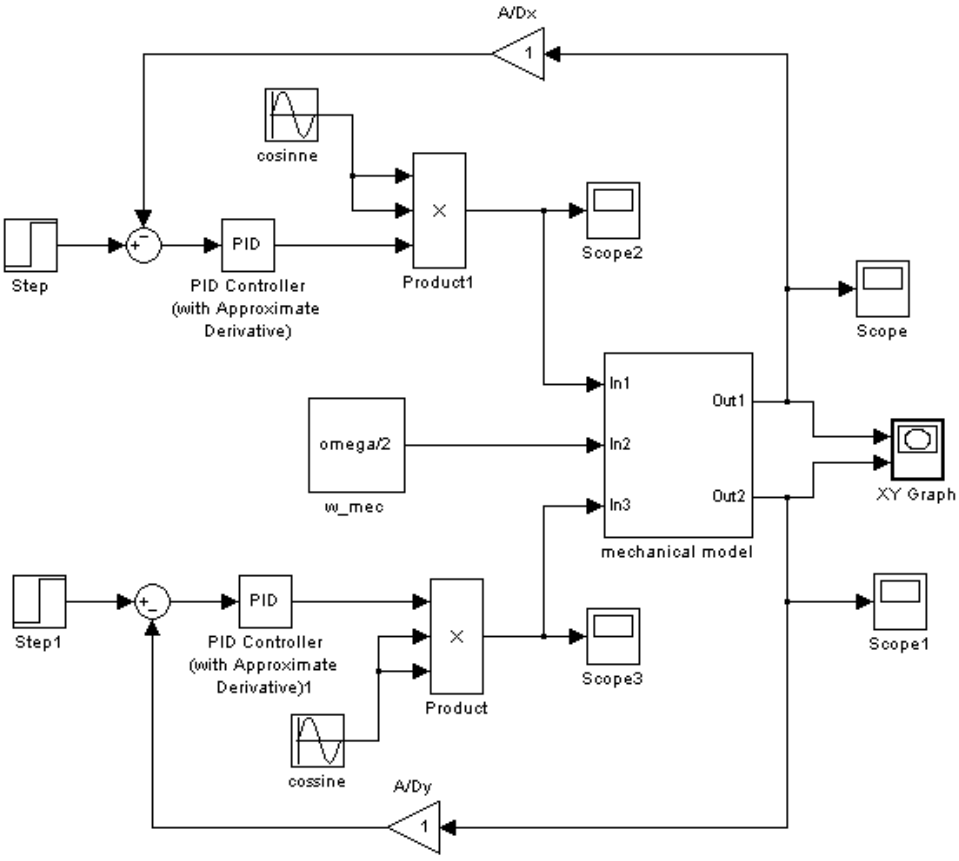

Figure 7. Diagram model of the control system.

The proposed mechanical model takes into account gyroscopic coupling given by omega (Ω). For low speeds, this coupling has low effect. This assumption allows the design of independent PD controllers for each positioning axis.

Figure 8 shows the simulation results for different speeds. The effect of rotor speed on transient responses of the position control may be observed with these results.

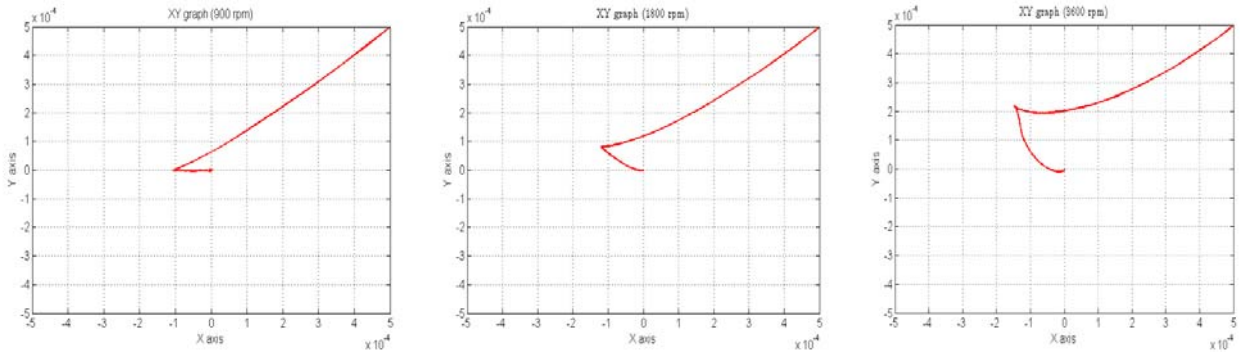

(a) (b) (c)

Figure 8. Simulated transient responses (initial condition x=0.5mm, y=0.5mm)
a) 900 rpm, b) 1800 rpm, c) 3600 rpm.

Simulations can be carried out to compare the effect of the proportional and derivative parameters in the system behavior. Figure 9 shows some results, for omega (Ω) equal to 377 rad/s, where position step responses can be seen for variations of the proportional (P) and the derivative (D) parameters.

The controller transfer function is given by:

$$C(s) = K_P\left[1 + \frac{\tau_D s}{(\tau_D/100)s + 1}\right] \tag{23}$$

where: $P = K_P$, and $D = K_P \cdot \tau_D$ are the proportional and derivative parameters, respectively.

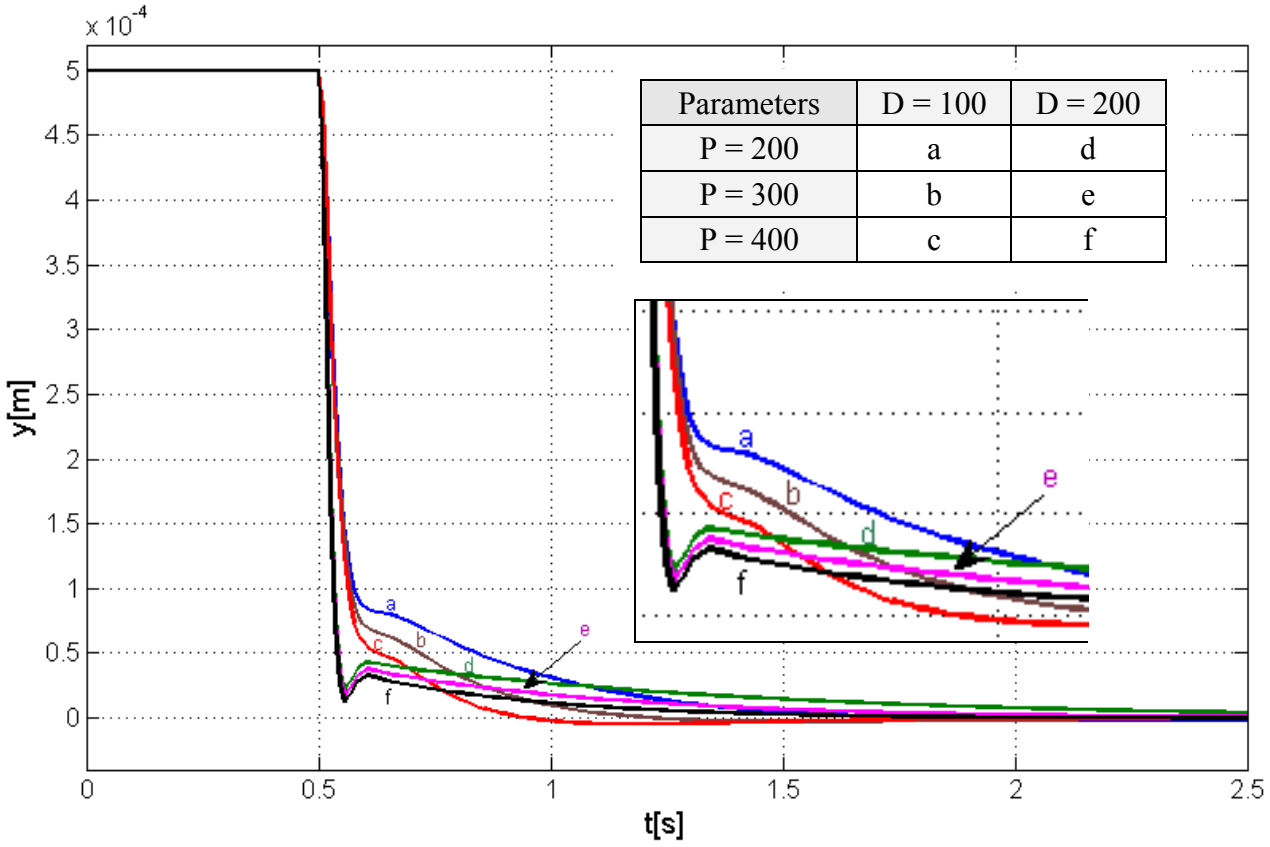

Figure 9: The steps responses for different controllers' parameters.

According to these simulations, controller "c" (P=400, D=100) presents the smallest settling time and no overshoot, being the best choice.

5. Conclusion

An electromagnetic and a mechanical model of a motor-bearing were proposed. Based on these models, simulation studies can be carried out to optimize the parameters of PD positioning controllers. The results presented in this paper will be tested in an experimental prototype in the near future.

6. Acknowledgements

The authors thanks to CNPq and CAPES for financial support.

7. References

Earnshaw S., 1842, "On the nature of the molecular forces which regulate the constitution of the luminiferous ether", Trans. Cambridge Phil. Soc. 7, 97-112.

David, D., Santisteban J. A., Del Nero Gomes A. C., Nikolsky, R., Ripper, A., 2003, "Dynamics and Control of a Levitating Rotor Suported by Motor Bearings", In: X International Symposium on Dynamic Problems of Mechanics, 2003, Ubatuba - SP. Proceedings of the X International Symposium on Dynamic Problems of Mechanics, Campinas - SP : ABCM - Brazilian Society of Engineering and Mechanical Sciences, 2003. v. 1. p. 283-288.

Santisteban J.A., Dadid, D., Noronha, R., Ripper, A., Stephan, R.M., 1997, "Controller Design for a Bearingless Electric Motor". In: 7th International Conference on Dynamic Problems in Mechanics, 1997, Angra dos Reis. 7th International Conference on Dynamic Probrlems in Mechanics, p. 169-171.

Santisteban J.A., Ripper, A., Stephan, R.M., David, D., Noronha, R., 1999, "Controller Design for a Bearingless Electric Motor. Revista Brasileira de Ciências Mecânicas", Brasil, v. XXI, n. 1, p. 91-98.

Santisteban, J. A., 1999, "Estudo da Influencia de uma Carga Torcional Sobre o posicionamento Radial de um Motor-Mancal", D.Sc. Thesis, COPPE/UFRJ, Rio de Janeiro, Brazil.

8. Responsibility notice

The authors are the only responsible for the printed material included in this paper.